Supporting Information

Crystal Structure Tuning in Organic Nanomaterials for Fast Response and High Sensitivity Visible-NIR Photo-detector

Taoyu Zou, Xiaoyan Wang, Haidong Ju, Qiong Wu, Tingting Guo, Wei Wu*, Hai Wang*
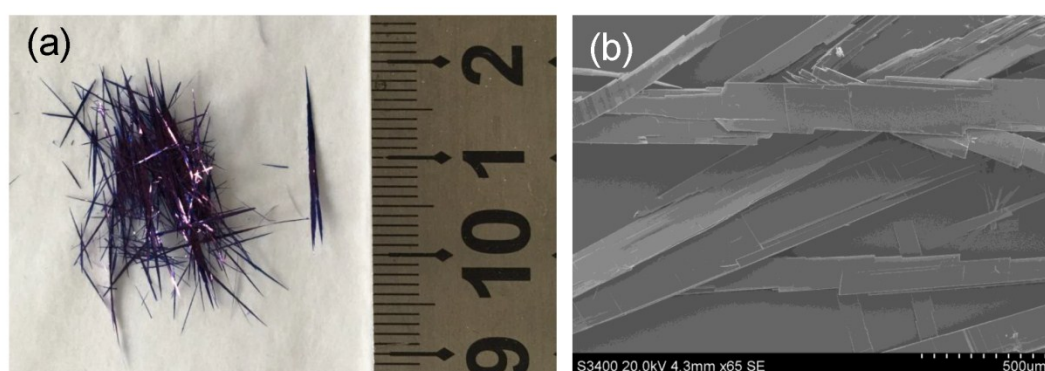
Fig. S1. (a) (b) Photograph and SEM of large size of ribbon-like $F_{16}CuPc$ crystal deposited in the high temperature zone.
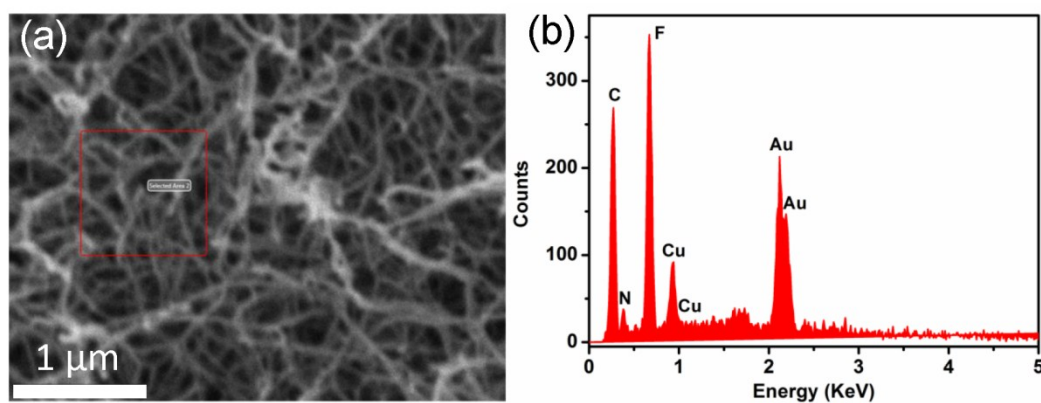
Fig. S2. a,b) $F_{16}CuPc$ nanowires on Si substrate and corresponding EDS spectrum.
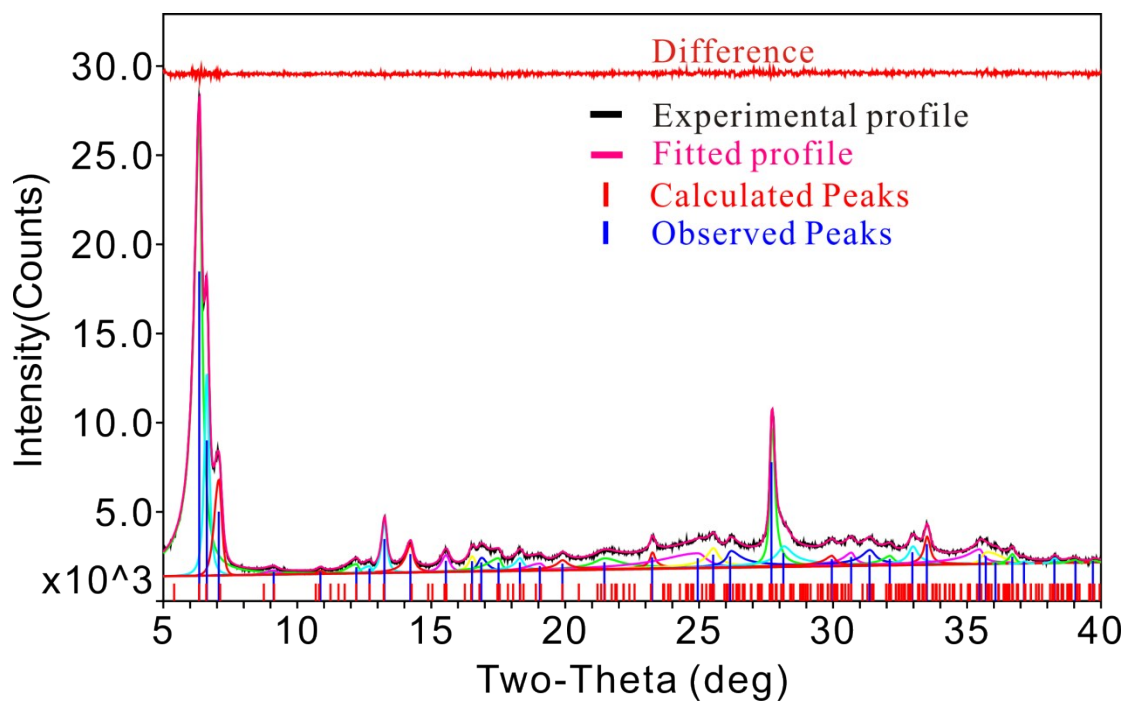
Fig. S3. Observed (black), fitted (pink), and difference (upper red line) X-ray powder diffraction patterns of $F_{16}CuPc$ nanowires. Vertical red lines refer to the position of all possible reflections; the observed peaks are marked with blue vertical lines. Residual Error of Fit (R) is 2.78%.

Table S1. Comparison between the fitted and calculated diffraction peaks and interplanar distance d (h k l), and corresponding lattice planes for $F_{16}CuPc$ nanowires.

2θ (°)			d (Å)			($h\,k\,l$)
Fitted	calculated	Δ (°)	Fitted	calculated	Δ (Å)	
6.346	6.338	0.008	13.9156	13.9343	-0.0187	(1 0 0)
6.626	6.602	0.024	13.3289	13.3781	-0.0492	(-1 0 2)
7.071	7.122	-0.051	12.491	12.4024	0.0886	(0 0 2)
9.120	9.132	-0.012	9.6885	9.6756	0.0129	(-1 0 3)
12.207	12.198	0.009	7.2446	7.2497	-0.0051	(-1 0 4)
13.253	13.225	0.028	6.6752	6.6891	-0.0139	(-2 0 4)
14.225	14.271	-0.046	6.2211	6.2012	0.0199	(0 0 4)
15.548	15.567	-0.019	5.6945	5.6876	0.0069	(-2 0 5)
16.525	16.49	0.035	5.3600	5.3712	-0.0112	(-3 0 2)
16.87	16.801	0.069	5.2512	5.2724	-0.0212	(-3 0 4)
17.516	17.551	-0.035	5.0590	5.0488	0.0102	(2 0 2)
18.310	18.323	-0.013	4.8413	4.8378	0.0035	(-2 0 6)
23.246	23.200	0.046	3.8233	3.8307	-0.0074	(-4 0 6)
27.701	27.734	-0.033	3.2177	3.2139	0.0038	(0 1 4)
28.143	28.151	-0.008	3.1681	3.1673	0.0008	(1 1 3)
30.678	30.676	0.002	2.9118	2.9121	-0.0003	(-3 0 10)
31.363	31.431	-0.068	2.8498	2.8438	0.006	(-4 0 10)
32.118	32.091	0.027	2.7845	2.7869	-0.0024	(5 0 0)
32.960	32.938	0.022	2.7153	2.7170	-0.0017	(-4 1 2)
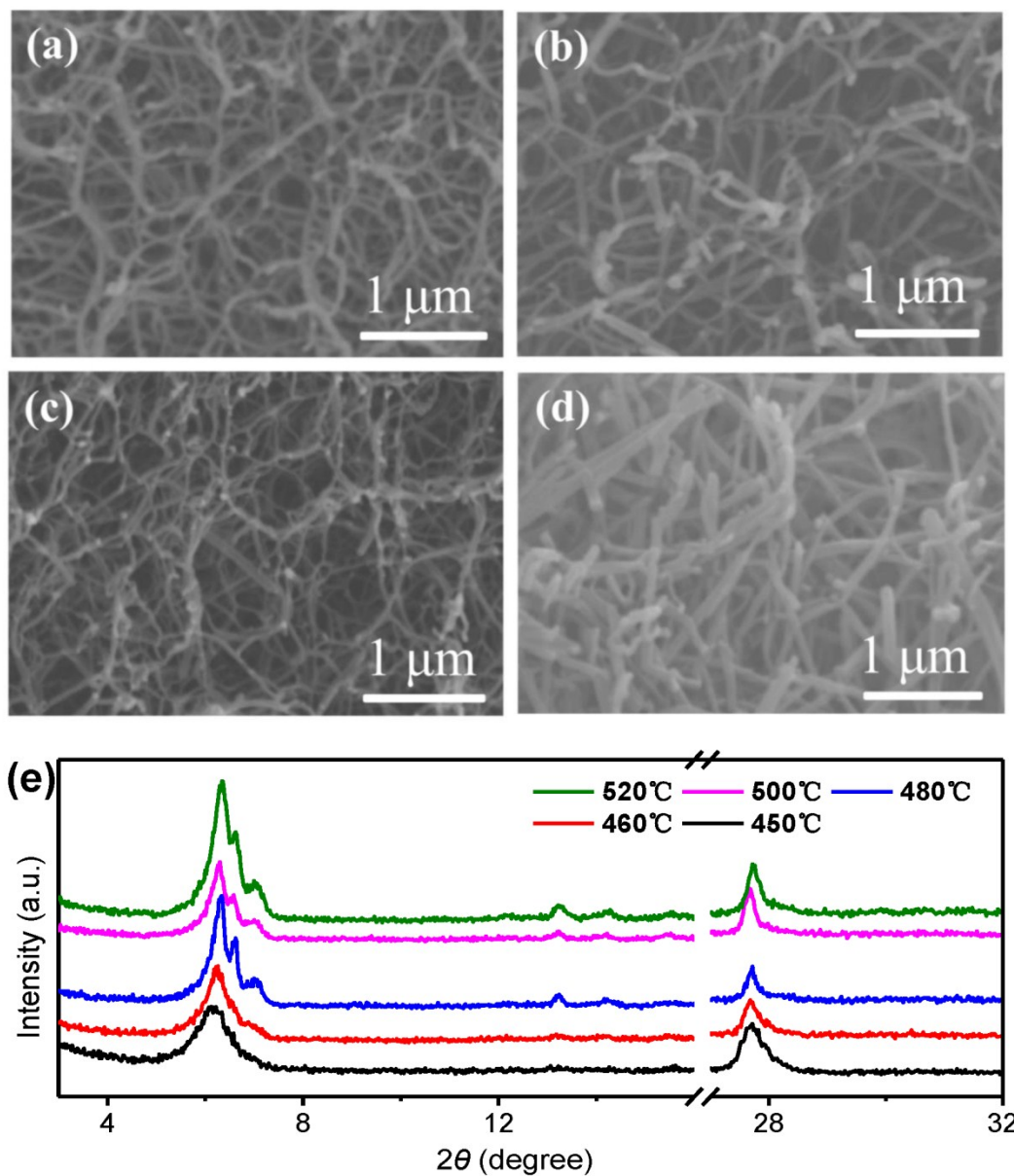
Fig. S4. SEM images for F16CuPc nanowires prepared at precursor temperature of a) 450 °C, b) 460 °C, c) 480 °C and d) 500 °C. e) XRD patterns for as-grown F16CuPc nanowires prepared at different precursor temperature ranging from 450 °C to 520 °C.
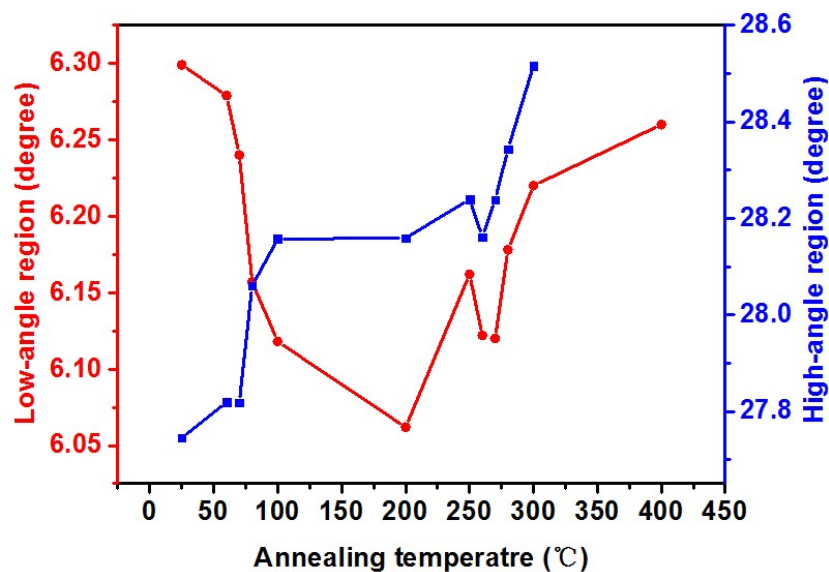
Fig. S5. Two feature diffraction peaks transition at low/high region along with the annealing temperature, respectively.
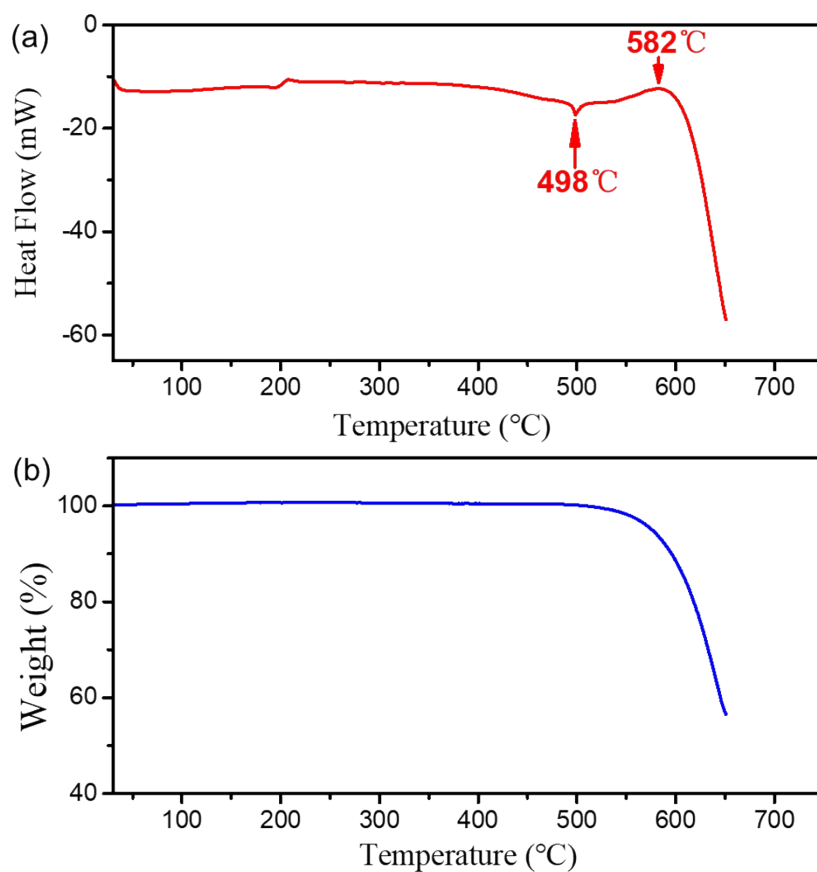
Fig. S6. a) DSC curves of $F_{16}CuPc$ nanowires at a heating rate of 20 °C /min in N_2 atmosphere, the peak at 498 °C indicated a complete transformation into β-phase. b) Thermogravimetric curve of $F_{16}CuPc$ nanowires and thermal vaporization starts at 582 °C.
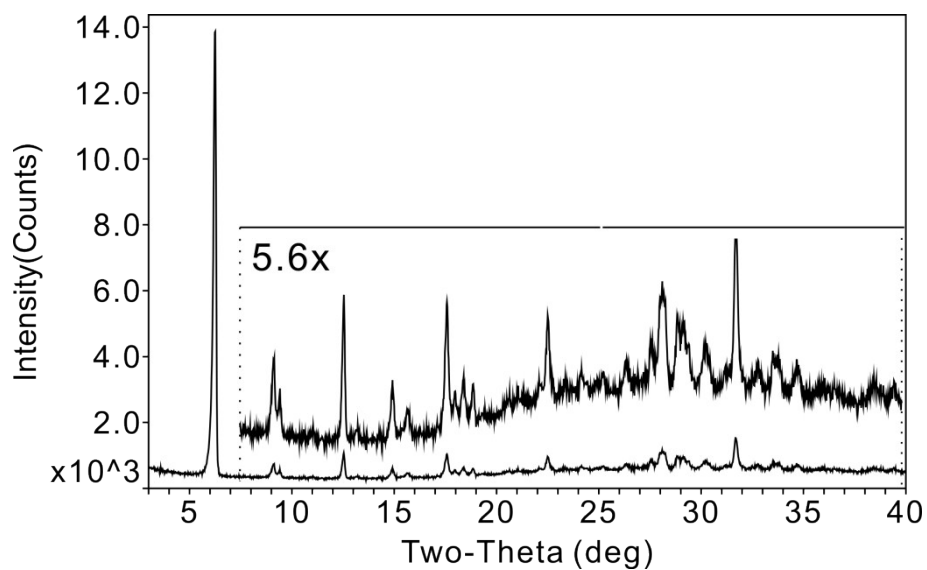
Fig. S7. The XRD pattern of the remaining sample for F16CuPc nanowires after DSC measurements up to 500 °C
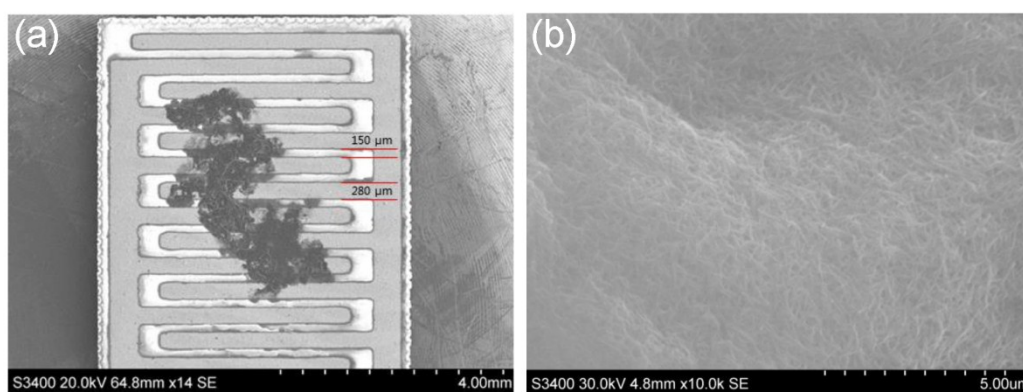
Fig. S8. a,b) SEM of photodetector and corresponding F16CuPc nanowires on the substrate.
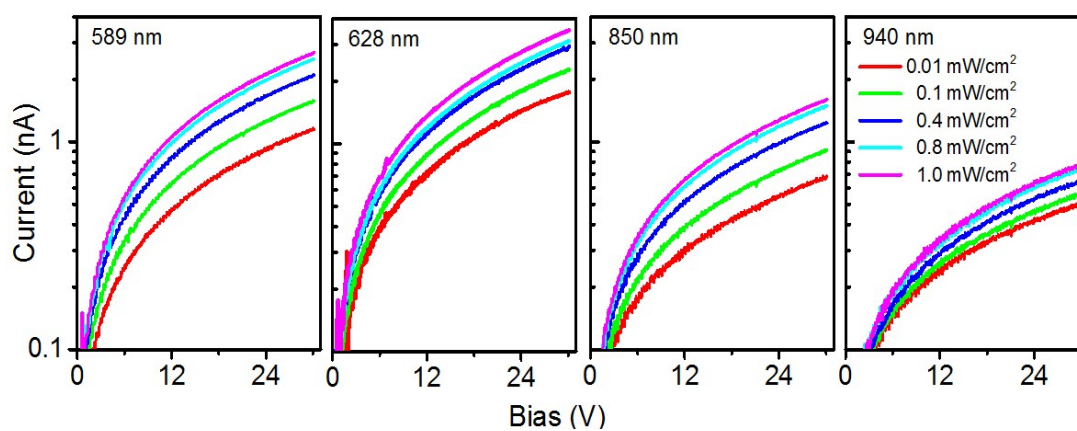
Fig. S9. I-V curve of the photodetector device under different LED laser emitting (589, 628, 850 and 940 nm) and light intensity.
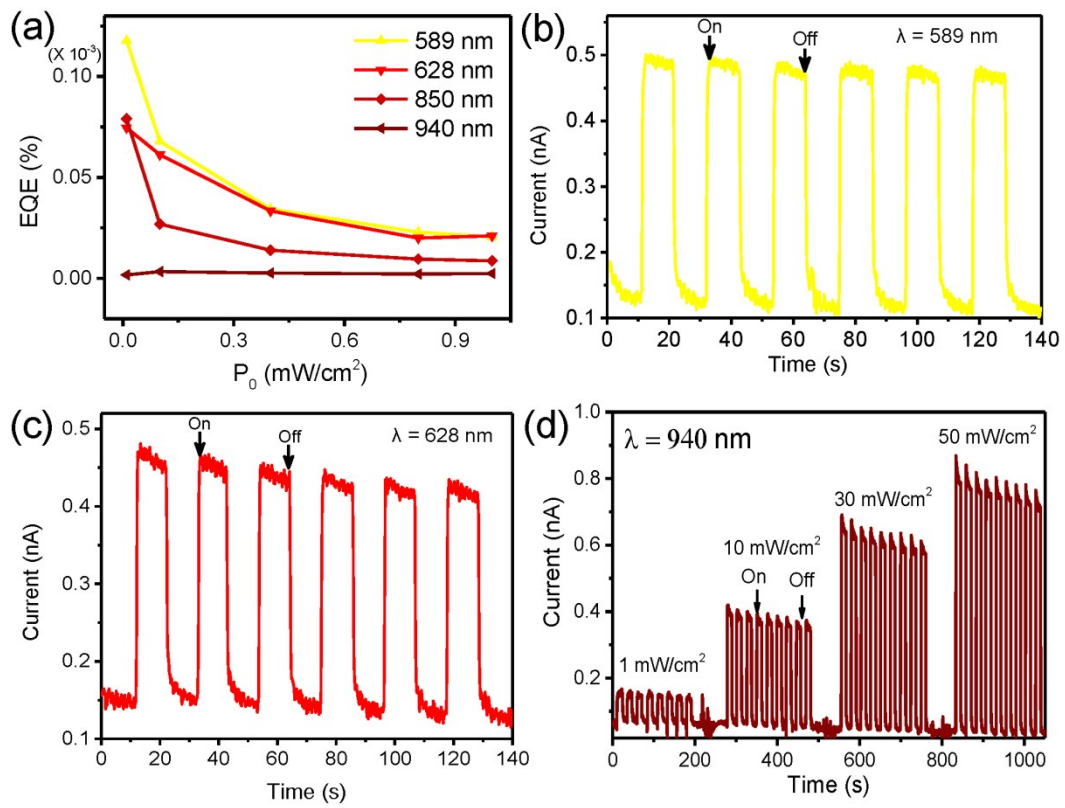
Fig. S10. a)The EQE of η-F$_{16}$CuPc nanowires based photodetector device versus light intensity under various wavelength illumination conditions; b,c) Photo response characteristics of the photodetector device for 589 and 628nm under light intensity 1mW/cm^2 at fixed bias 10V; d) Photo response characteristics to 940 nm light under different densities of incident light illumination at a fixed bias of 10 V.